Ionics (2022) 28:4303–4310
https://doi.org/10.1007/s11581-022-04647-8

ORIGINAL PAPER

Synthesis of poly(isobutylene-*alt*-maleic anhydride)-based water-soluble binders and their electrochemical properties

Seung-Taek Oh[1] · Ye-Won Jeong[1] · Sung-Soo Kim[2] · Sang-Woog Ryu[1]

Received: 24 May 2022 / Accepted: 12 June 2022 / Published online: 21 June 2022

Abstract

In this study, water-soluble polymer electrolytes were synthesized, and their potential as binders for negative electrode active materials was evaluated. Poly(isobutylene-*alt*-maleic anhydride) was used as a base material, and it was turned water-soluble via reaction with an excess of LiOH in the presence of maleic anhydride. In the next step, a BF_3-THF complex was introduced into the lithium carboxylate group, and the ionic conductivity of the polymer electrolyte was improved proportionately by the amount of Lewis acid incorporation. The synthesized water-soluble polymer electrolyte was mixed with SBR and used as a binder for an anode active material. Although the peel strength decreased as the content of the polymer electrolyte binder increased, the lithium-ion battery composed of Li/electrolyte/graphite showed relatively high formation efficiency. In particular, the improvement in cell performances was observed because the resistance of the negative electrode interface was reduced by the ion conductive polymer binder.

Keywords Polymer electrolytes · Water soluble · Binder · Peel strength · Interfacial resistance

Introduction

Lithium-ion secondary batteries have excellent characteristics such as high energy density, low self-discharge, and large electromotive force; thus, they are widely used in mobile phones, notebook computers, electric bicycles, electric vehicles, and energy storage systems (ESS) [1–3]. In particular, the demand for lithium batteries with higher capacity and safety is increasing significantly as it is widely applied to new industrial fields such as autonomous vehicles, delivery drones, aerial vehicle, and marketing robots [4–7]. It is well known that lithium-ion secondary batteries are composed of positive and negative electrode, separator, and electrolyte [8]. Furthermore, the negative and positive electrodes are composed of metal current collector, active material, conductive agent, and binder, respectively. Among them, the binder plays a very important role in mechanically stabilizing the electrode by utilizing its own adhesive force [9–13]. Practically, the graphite electrode repeats 10% of expansion and contraction as the lithium-ion intercalation–deintercalation reaction proceeds. In this process, the contact resistance between the particles increases if the bond between the active materials is deformed and the cell performance decreases [14–16]. In this regard, poly(vinylidene fluoride) (PVDF) and styrene-butadiene rubber (SBR)/carboxymethyl cellulose (CMC) are fairly used as positive and negative binders, respectively [17–19]. In addition to PVDF or SBR, a study on the capacity and cycle improvement of batteries using poly(sodium acrylate) grafted carboxymethyl cellulose, poly(acrylic acid), and poly(vinyl alcohol)-based binders for silicon anodes has been reported [20, 21]. However, investigation of the binders for negative electrodes using ion conductive polymers has not been extensively carried out. As the above-mentioned PVDF or SBR-based binders do not have ionic conductivity, they act as resistive materials in the process in which lithium ions are intercalated into or deintercalated from graphite. Therefore, if the ion conductive polymer electrolyte is used as a binder, the resistance in the electrode can be reduced, leading to the improvement of the performance and cycle of the battery [22–25]. However, several conditions need to be made in order to use the ion conductive polymer for binder

✉ Sang-Woog Ryu
swryu@chungbuk.ac.kr

[1] Department of Engineering Chemistry, College of Engineering, Chungbuk National University, Cheongju 28644, Chungbuk, Korea

[2] Graduate School of Energy Science and Technology, Chungnam National University, Daejeon 305-764, Korea

applications, particularly for negative electrodes. First, the polymer electrolyte binder must have both ionic conductivity and adhesive properties. Second, a water-soluble polymer is required like the SBR system that is currently applied to the anode electrode. Third, the polymer must have single ion conduction properties in order to prevent polarization of the lithium salt in the entire binder [26–28]. Therefore, development of a water-soluble polymer electrolyte, which can satisfy these conditions, will lead to next-generation battery materials [29].

The purpose of this study is to synthesize poly(isobutylene-*alt*-maleic anhydride) (PIMA)-based water-soluble polymer electrolyte (PIMA-Li) and to investigate the correlation between ionic conductivity, binding force, and interfacial resistance in terms of the content of polymer electrolyte. To achieve this purpose, the conditions for water solubility change of PIMA were explored, and ionic conductivity was observed by introducing the BF_3-THF complex additive. In addition, a slurry made by mixing the as-synthesized polymer electrolyte and SBR was coated on copper foil to fabricate electrodes with different polymer electrolyte contents, and peel strength and interfacial properties were investigated.

Materials and methods

Materials

PIMA (average MW = 6000 g/mol, Aldrich) and LiOH (99%, Aldrich) were used without further purification. Tetrahydrofuran (THF, 99.5%), ethanol (95%), acetone (99.5%), *N*, *N*-dimethylformamide (DMF, 99.5%), hexane (95%), and dimethyl sulfoxide (DMSO, 99.8%) were supplied from Samchun Co., and toluene (99.9%) was purchased from Aldrich. Boron trifluoride tetrahydrofuran complex (BF_3-THF complex, Aldrich) was used without purification. The electrolyte used for absorption test and battery preparation is EC/DEC (1/1, v/v, Panax Starlyte) in which 1 M of LiTFSI is dissolved. SBR and CMC that were used to prepare binder slurry were supplied by Hansol Chemical Co.

Preparation of polymer electrolytes

The synthesis of PIMA-Li and PIMA-Li-BF_3 was carried out through a two-step reaction process and is shown in Fig. 1. The detailed preparation process of PIMA-Li is as follows. After dissolving 8 g (333 mmol) of LiOH in 60 mL of distilled water, the temperature of the reactor was increased to 90 °C, and 15 g (2.5 mmol) of PIMA was added to the reactor, and the temperature was maintained for 24 h. After the reaction was completed, the polymer solution dissolved in water was concentrated through an evaporator (rotary evaporator, TOKYO RIKAKIKAI, N-100) and precipitated in excess ethanol. The precipitated polymer was placed in a vacuum dryer and dried at 65 °C for 24 h to obtain PIMA-Li in powder form. To prepare PIMA-Li-BF_3 in the next step, 1.86 mL (16.7 mmol) of BF_3-THF complex and 2 g (0.28 mmol) of PIMA-Li were added to an 85 °C reactor in which 30 mL of DMSO was introduced. After 24 h, the polymer solution was poured into a large amount of acetone and vacuum dried at 60 °C for 24 h to obtain PIMA-Li-BF_3 in powder form. Electrolyte absorption of the synthesized PIMA-Li-BF_3 was calculated by measuring the difference in weight before and after adding 0.1 g of a polymer electrolyte

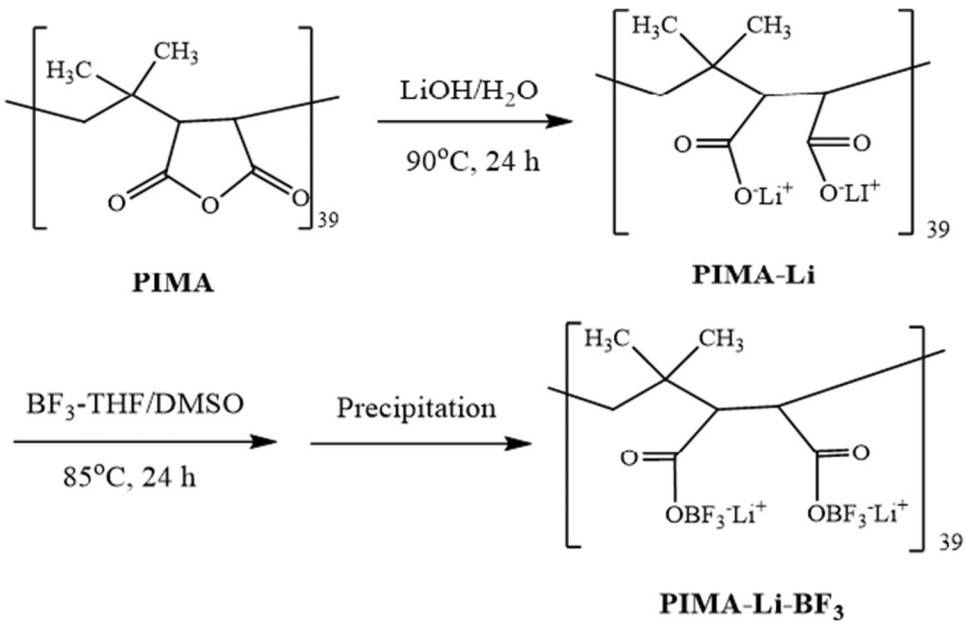

Fig. 1 Synthetic procedure for PIMA-Li-BF_3

to the liquid electrolyte at 25 °C and impregnating it for 24 h.

Half-cell fabrication

The half-cell preparation for evaluating the battery performance was carried out as follows. As a first step, a mixed binder was prepared by adding the synthesized PIMA-Li-BF_3 to SBR in the amounts of 5, 10, or 15 wt%. Next, graphite, CMC, and the prepared binder were mixed in a ratio of 97.5:1.0:1.5 wt% to make a slurry, and finally, it was coated on copper foil and dried at 100 °C for 20 min. The electrode density of the prepared negative electrode was 1.7 g/cm^3, and a half-cell was prepared using lithium foil as a counter electrode.

Characterization

Chemical changes of the polymer before and after the reaction were analyzed by ^{1}H-NMR (Bruker DPX, 500 MHz) and FT-IR spectroscopy (JASCO Co. 480 plus). AC impedance and ionic conductivity of the polymer electrolyte were measured in a frequency range of 1 Hz to 1 MHz using potentiostat (1470E Multichannel Cell-test system, Solatron). Polymer electrolyte was placed in a stainless-steel symmetric cell with a diameter of 1.0 cm and a thickness of 0.1 cm before the measurement and heated at 85 °C for 2 h. The battery was assembled in CR 2016 type coin cell, and graphite was used as the negative electrode and lithium metal as the counter electrode. The charge/discharge characteristics were measured using a battery cycler (Battery Cycler system, WBCS3000) at 25 °C. The peel strength measurement of the polymer binder was conducted according to ASTM D882 [30]. More specifically, the negative electrode slurry with a width of 15 mm and length of 30 mm was coated on a 70-mm long copper plate and dried. Thereafter, the specimen was folded in half and compressed at 100 °C for 2 min prior to the tensile strength measurement using a Universal Testing Machine (UTM, Instron Instrument 3344R1742) at 25 °C.

Results and discussion

Preparation of water-soluble polymer electrolytes

Poly(isobutylene-*alt*-maleic anhydride) (PIMA) is an alternating copolymer which does not dissolve in water by itself [31]. However, as the maleic anhydride group can react with a basic reagent, it can be substituted with two lithium carboxylates by reaction of LiOH, as shown in Fig. 1. In this study, conversion into water-soluble polymers was measured by introducing various amounts of LiOH based on the concept mentioned above, and the results are summarized in Table 1. Depending on the maleic anhydride (MA) group of the polymer, the polymer produced at MA and LiOH molar ratio of 1:0.7 was not soluble in water; however, it started to become partially soluble from the ratio of 1:1 as the amount of LiOH introduction was slightly increased. Therefore, it was possible to measure the amount of polymer soluble in water from the ratio of 1:1, and in this case, a yield of 78% was observed. Similarly, in experiments where excess of LiOH (2 and 3.4 times compared to that of maleic anhydride) was used, highly water-soluble polymers with yields of 87% and 94% were obtained, respectively. Therefore, it is necessary to introduce 3.4 times or more of LiOH to reduce experimental error because it is a reaction in which 2 mol of LiOH is consumed for 1 mol of maleic anhydride. Figure 2 shows the results of ^{1}H-NMR measurement before and after the reaction between maleic anhydride and LiOH. In the case of PIMA, the alkyl (A) and (B) peaks at 3.29 and 3.10 ppm were split and shifted to (a) 2.78, 2.71 and (b) 2.44, 2.38 ppm, respectively after LiOH was added (P-2). This is because the structure of anhydride was converted to –COO$^-$Li$^+$ by the reaction of LiOH and PIMA. In addition, –COOH formed as an intermediate may co-exist with

Table 1 Feed ratio for the reaction between PIMA and LiOH

Run	MA (mmol)	LiOH (mmol)	Mole ratio (MA/LiOH)	Yield[a] (%)
P-1	32.5	21.5	1:0.7	Insoluble
P-2	32.5	32.5	1:1.0	78
P-3	32.5	65.0	1:2.0	87
P-4	97.5	333.3	1:3.4	94

[a]Collect the parts that are soluble in water

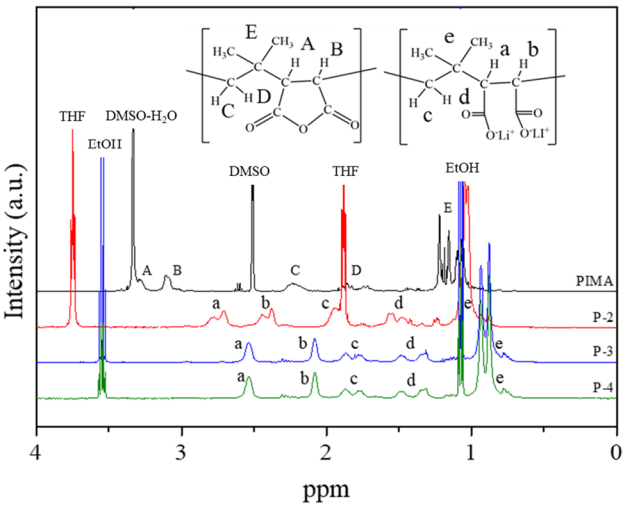

Fig. 2 ^{1}H-NMR spectra of PIMA and PIMA-Li in DMSO-*d6* and D_2O respectively

–COO^-Li^+ because it did not react with sufficient LiOH. Perhaps this is the reason why the NMR peak splits into two. From this point of view, most of the maleic anhydrides can be substituted with –COO^-Li^+ without –COOH in P-3 and P-4 where sufficient LiOH is used. As a result, (a) and (b) appeared as single peaks at 2.54 and 2.08 ppm, respectively. Interestingly, the peaks (c) and (d) from isobutylene are clearly separated at 1.87, 1.77 ppm, and 1.49, 1.32 ppm, respectively after –COO^-Li^+ substitution of the adjacent anhydride. Although the peaks appear separated as described above, the integral ratio of the (a), (b), (c), and (d) peaks in P-4 is 1.00:0.99:1.01:1.07, respectively. Therefore, it can be said that PIMA was quantitatively converted into PIMA-Li.

The reaction of –COO^-Li^+ and BF_3-THF in a polymer electrolyte is frequently carried out for improving ionic conductivity [32, 33]. In this study, an experiment was conducted to introduce BF_3-THF into PIMA-Li for the similar purpose, and Fig. 3 shows the FT-IR measurement results before and after the reaction. In PIMA itself, distinct C = O peaks can be identified at 1780 and 1856 cm^{-1} which are corresponded to anhydride. However, the anhydride disappears by reacting with LiOH, and instead, a peak related to –COO^-Li^+ is observed at 1580 cm^{-1}. Of course, the C = O group peak that still exists after the reaction should appear, but it is not observed clearly because it is covered to the –COO^-Li^+ peak having a relatively high absorption intensity. In the next step, as BF_3-THF is introduced into PIMA-Li, the –COO^-Li^+ peak at 1580 cm^{-1} is reduced, and a new –COO $BF_3^-Li^+$ peak is observed at 1728 cm^{-1} [32]. At the same time, the peaks at 1780 and 1856 cm^{-1} related to C = O also reappeared. Therefore, it is confirmed that PIMA was replaced with PIMA-Li and finally converted into PIMA-Li- BF_3. In this experiment, $(–COO)_2BFLi$ may be formed by intermolecular reaction so there may be a possibility of forming a cross-linked product, but it is thought that such reaction did not proceed because the final synthesized PIMA-Li-BF_3 was well dissolved in the solvent. The amount of BF_3-THF introduction was adjusted to 1–77% with respect to the amount of –COO^-Li^+ in this experiment and the detailed composition is shown in Table 2. In addition, more than 77% of BF_3-THF was not introduced because it may negatively affect battery performance due to its corrosiveness if unreacted BF_3 exists in excess. Meanwhile, Table 3 shows the changes in solubility for PIMA, PIMA-Li, and PIMA-Li-BF_3 samples. PIMA was soluble only in DMF and DMSO but showed solubility in H_2O as it was substituted with lithium salt. Finally, it showed solubility in both H_2O and DMSO as BF_3-THF was introduced.

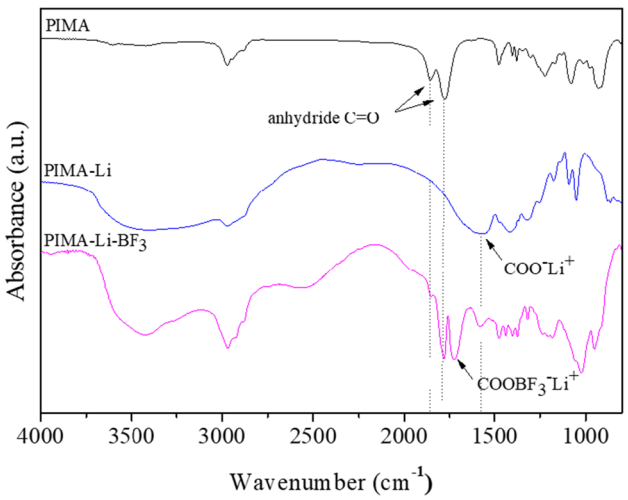

Fig. 3 FT-IR spectra of PIMA, PIMA-Li (P-4 in Table 1), and PIMA-Li-BF_3 (T-5 in Table 2)

Physical and electrochemical properties of polymer electrolytes

When the polymer electrolyte is used as a binder of the electrode active material, the physicochemical properties are changed in contact with the liquid electrolyte. In particular, it is expected to exhibit different electrochemical behavior from that of SBR in the case of an ionic conductive polymer electrolyte because it can absorb the liquid electrolyte [34, 35]. In this study, the electrolyte absorption behavior of the polymer electrolyte was investigated using EC/DEC (1/1, v/v) with 1 M LiTFSI, and the results are shown in Fig. 4. As expected, the amount of electrolyte absorption increases with the increase in amount of BF_3-THF. Thus, 133% of electrolyte absorption was observed when BF_3-THF was introduced at 77 mol% equivalent. In addition, it is assumed

Table 2 Compositions for complex formation between –COOLi group and BF_3

Run	–COOLi[a] (mmol)	BF_3-THF (mmol)	Mole ratio (–COOLi:BF_3-THF)	Amount of BF_3-THF introduced (%)
T-1	32.7	0.42	1:0.01	1
T-2	21.8	0.55	1:0.03	3
T-3	21.8	2.24	1:0.10	10
T-4	21.8	5.6	1:0.26	26
T-5	21.8	16.7	1:0.77	77

[a]The polymer is a sample indicated as P-4 in Table 1

Table 3 Solubility test of polymers in various solvents

Polymer	Toluene	THF	DMF	DMSO	H_2O
PIMA	×	×	O	O	×
PIMA-Li	×	×	×	×	O
PIMA-Li-BF_3	×	×	×	O	O

[a]O soluble, × insoluble at 25 °C

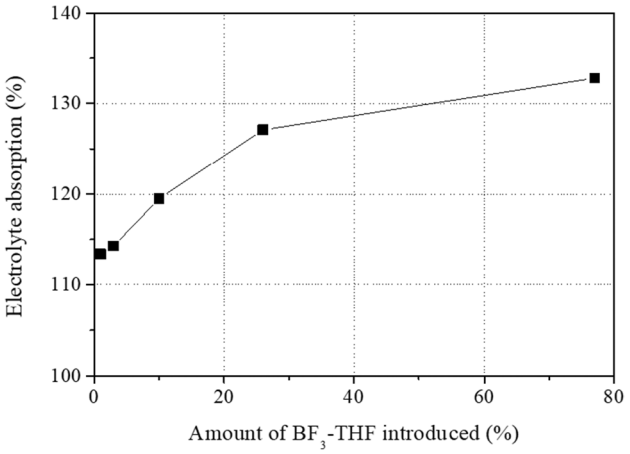

Fig. 4 Electrolyte absorption of PIMA-Li-BF_3 polymer electrolytes according to the amount of BF_3-THF introduced at 25 °C

that a certain amount of electrolyte absorption may occur even in the PIMA-Li sample in which its own lithium salt exists. However, despite these advantages, problems such as volume expansion and reduction in binding force may also occur if the electrolyte is excessively absorbed. Therefore, it is necessary to properly mix PIMA-Li- BF_3 with SBR binder to obtain bonding strength while maintaining ionic conductivity. In contrast, the PIMA-Li- BF_3 synthesized in this study can have high ionic conductivity when the electrolyte is absorbed, but because it was obtained in powder form, lithium-ion movement at room temperature is not easy. Considering these characteristics, the ionic conductivity was measured at 85 °C instead of room temperature, and the results are shown in Fig. 5. In fact, lithium carboxylate has a strong ionic bond with each other, so it is difficult to expect high ionic conductivity by itself. In particular, ionic conductivity close to that of an insulator will be observed if

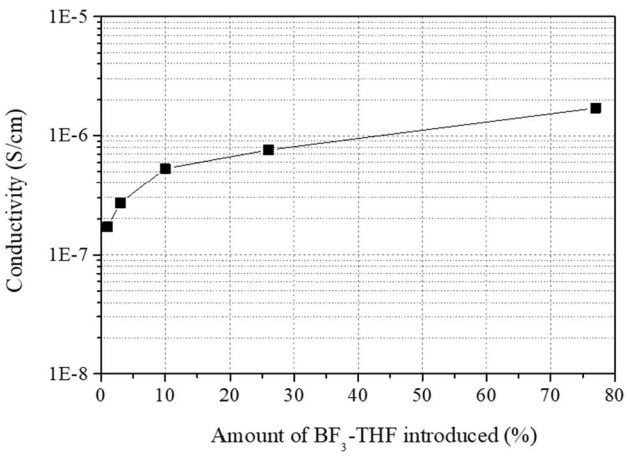

Fig. 5 Ionic conductivity of polymer electrolytes according to the amount of BF_3-THF introduced at 85 °C

the polymer is in the form of a powder [36, 37]. Therefore, more free movement of lithium ions is possible by lowering the ionic bond strength via introduction of BF_3-THF. In this experiment, it was found that the ionic conductivity increased as the amount of BF_3-THF used for PIMA-Li increased. As a result, the ionic conductivity of 1.7×10^{-7} S/cm was obtained at 1% BF_3-THF introduction, whereas it increased ten times to 1.7×10^{-6} S/cm at 77% BF_3-THF introduction.

As described above, PIMA-Li- BF_3 cannot be applied alone as a binder because it absorbs electrolyte. For that reason, a slurry was prepared by mixing PIMA-Li-BF_3 and SBR. Then, the peel strength was tested by coating it on copper foil [38, 39], and the results are shown in Table 4. B-0 is a binder used only with SBR, and binders using 5, 10, and 15 wt% of PIMA-Li-BF_3 (T5 sample in Table 2) are indicated as B-5, B-10, and B-15, respectively. Unfortunately, an adhesive strength of 71 kPa was observed when 15 wt% of the polymer electrolyte was used, which was calculated to be 42% of that of the SBR-only binder. Therefore, the adhesive strength decreases as the amount of added polymer electrolyte increases. However, a relatively high peel strength of 133 kPa was observed in the B-5 sample using only 5 wt% of the polymer electrolyte, which is 79% of that of the SBR binder and is expected to be applicable to actual battery applications.

Cell performance

The mixed binder composed of the synthesized polymer electrolyte and SBR was applied to a negative electrode assembly using graphite as an active material, and cell performance was evaluated through a half-cell using metallic lithium as a counter electrode. As described above, the mixed binder contained 5(B-5), 10(B-10), and 15(B-15) wt% of polymer electrolyte and was compared with the 100% SBR sample (B-0). Figure 6 shows the first charge/discharge voltage profile of the half-cell using binders of various compositions. In terms of discharge capacity, B-0 using 100% SBR showed 313 mAh/g, whereas B-5, B-10, and B-15 showed improved results to 338, 340, and 328 mAh/g, respectively.

Table 4 Composition of binder for negative electrode and peel strength

Run	Weight (%)		Peel strength (kPa)
	SBR	PIMA-Li-BF_3[a]	
B-0	100	0	169
B-5	95	5	133
B-10	90	10	93
B-15	85	15	71

The polymer is a sample indicated as T-5 in Table 2

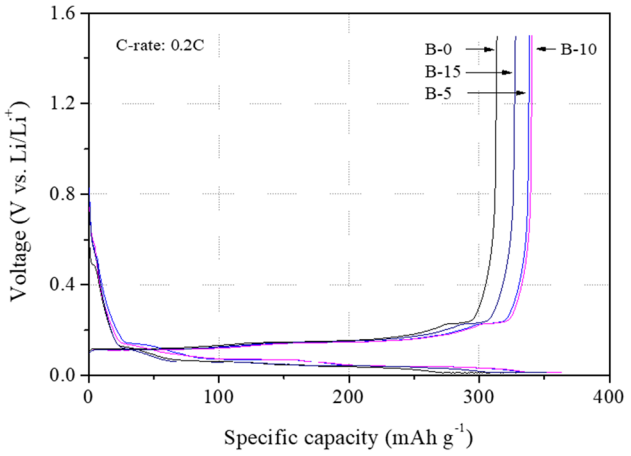

Fig. 6 Charge/discharge voltage profiles of half-cells using various binders for negative electrodes

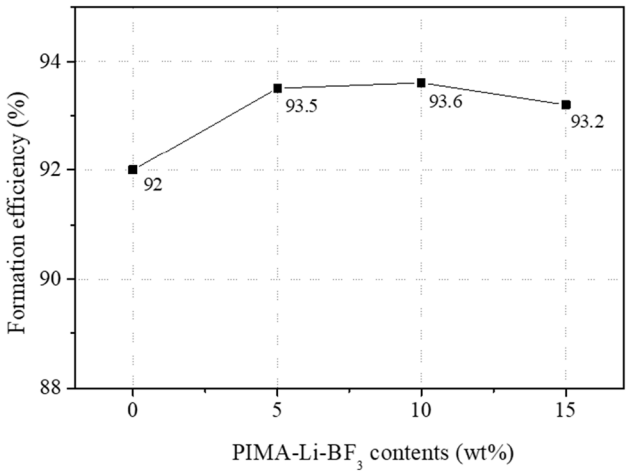

Fig. 7 Formation efficiency of half-cells prepared by varying the amount of polymer electrolyte binder for negative electrode

Interestingly, a higher discharge capacity was observed in the binder containing 10 wt% of the polymer electrolyte compared to the sample containing 15 wt% of the polymer electrolyte. Although improvement in ionic conductivity can lead to an increase in discharge capacity, maintaining the adhesive strength of the anode active material is also important for maintaining battery performance. Therefore, based on the adhesion and initial discharge capacity tests, the binder containing 5 wt% of polymer electrolyte is the optimal composition in this study. Meanwhile, the first charge/discharge is a process that stabilizes the battery structure and forms a solid electrolyte interphase (SEI) layer on the surface of the anode, which is important for maintaining battery performance [40–42]. In this process, the difference between charge and discharge capacity is called formation efficiency, and the battery capacity can be reduced when lithium-ion consumption is large. Figure 7 shows the formation efficiency according to the polymer electrolyte content. It can be clearly seen that the presence of the ion conductive polymer electrolyte in the electrode improves the efficiency [43, 44]. As a result, up to 93.6% of formation efficiency was obtained in B-10. As a binder, the ionic conductive polymer electrolyte can be expected to play a role in lowering the interfacial resistance as well as promoting the movement of lithium ions. Compared to SBR, the polymer electrolyte has affinity with the electrolyte; therefore, it is considered that the movement of the electrolyte to the active material is relatively easy. To confirm this further, the AC impedance of the half-cell using binders of various compositions was measured, and the results are shown in Fig. 8. As the battery consists of the lithium metal counter electrode and the graphite negative electrode, the resistance component can be interpreted in the order of the resistance of the cell itself, the negative electrode interface, and the lithium interface as shown in the equivalent circuit. The total resistance which is the sum of the interfacial resistance of the negative and the lithium electrode decreases as the content of the ionic conductive polymer electrolyte increases. Among them, the resistance of the anode interface to which the polymer electrolyte is applied is separated and shown in Fig. 9. As a result, it can be clearly observed that the negative electrode interfacial resistance is decreased in contrast to the amount of the polymer electrolyte used. This may be due to the reduced decomposition on the surface of the active material owing to the mobility of lithium ions and absorption of the electrolyte. Therefore, if the ion conducting polymer electrolyte is used as a binder, the capacity is increased and the interfacial resistance is decreased due to the movement of lithium ions and absorption of the electrolyte. However, additional research is needed to maintain the adhesive strength between active materials during battery operation.

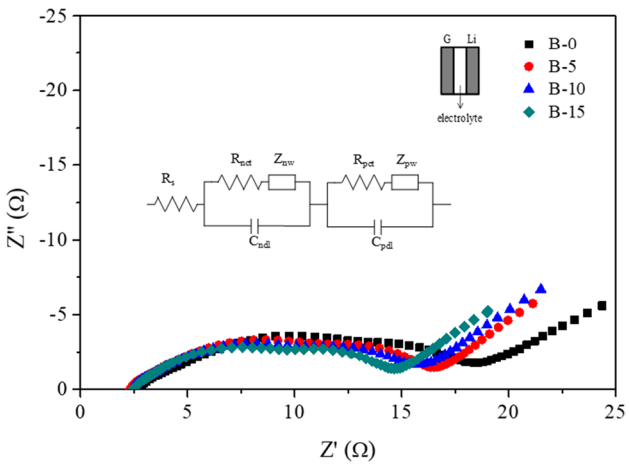

Fig. 8 Nyquist plot of half-cell according to the amount of polymer electrolyte binder

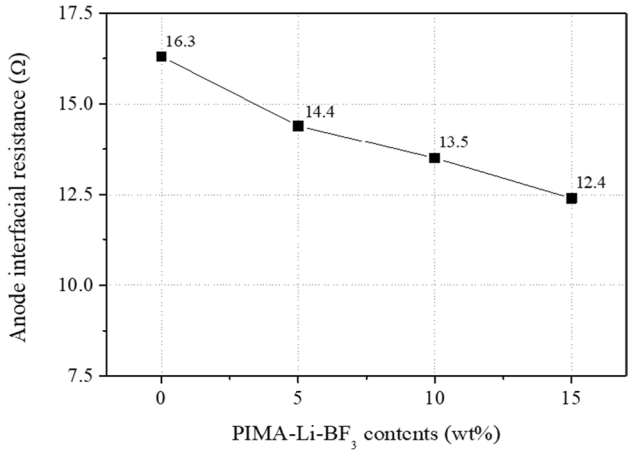

Fig. 9 Changes in anode interfacial resistance according to the amount of PIMA-Li-BF_3

Conclusion

In this study, water solubility was obtained by substituting PIMA with PIMA-Li as the starting material. Specifically, water-insoluble PIMA was converted into a water-soluble polymer by reacting with LiOH and was dissolved in both water and DMSO after additional introduction of BF_3-THF. The absorption of the liquid electrolyte into the synthesized polymer electrolyte increased as the amount of BF_3-THF increased, and the ionic conductivity measured at 85 °C showed a similar trend. In contrast, it was observed that as the amount of PIMA-Li-BF_3 added to the SBR binder increased, the adhesion strength to the copper electrode decreased. However, at the same time, it was confirmed that the formation efficiency was increased, and the interfacial resistance of the anode active material was greatly reduced. Therefore, it is expected to show an improved battery performance while providing an appropriate level of adhesion when about 5 wt% of PIMA-Li-BF_3 is added to the SBR binder.

Funding This research was supported by Chungbuk National University, Korea National University Development Project (2021).

References

1. Dias F, Polomp L, Veldhuis J (2000) Trend in polymer electrolytes for secondary lithium batteries. J Power Sources 88:169–191
2. Tarascon J, Armand M (2001) Issues and challenges facing rechargeable lithium batteries. Nature 414:359–367
3. Lee J, Lee Y, Bhattacharya B, Nho Y, Park J (2009) Separator grafted with siloxane by electron beam irradiation for lithium secondary batteries. Electrochim Acta 54:4312–4315
4. Jung S, Jeong H (2017) Extended Kalman filter-based state of charge and state of power estimation algorithm for unmanned aerial vehicle Li-Po battery packs. Energies 10:1237
5. Hollinger AS, McAnallen DR, Brockett MT, DeLaney SC, Ma J, Rahn CD (2020) Cylindrical lithium-ion structural batteries for drones. Int J Energy Res 44:560–566
6. König A, Nicoletti L, Schröder D, Wolff S, Waclaw A, Lienkamp M (2021) An overview of parameter and cost for battery electric vehicles. World Electr Veh J 12:21
7. Liu Y, Zhang R, Wang J, Wang Y (2021) Current and future lithium-ion battery manufacturing. IScience 24:102332
8. Van Schalkwijk W, Scrosati B (2002) Advances in lithium-ion batteries. Kluwer Academic/Plenum, New York
9. Pender J, Jha G, Youn D, Ziegler J, Andoni I, Choi E, Heller A, Dunn B, Weiss P, Penner R, Mullins C (2020) Electrode degradation in lithium-ion batteries. ACS Nano 14:1243–1295
10. Landesfeind J, Eldiven A, Gasteiger H (2018) Influence of the binder on lithium ion battery electrode tortuosity and performance. J Electrochem Soc 165:A1122–A1128
11. Shi Y, Zhou X, Yu G (2017) Material and structural design of novel binder systems for high energy, high-power lithium-ion batteries. Acc Chem Res 50:2642–2652
12. Jiang M, Mu P, Zhang H, Dong T, Tang B, Qiu H, Chen Z, Cui G (2022) An endotenon sheath-inspired double-network binder enables superior cycling performance of silicon electrodes. Nano-Micro Lett 14:87
13. Mu P, Zhang H, Jiang H, Dong T, Zhang S, Wang C, Li J, Ma Y, Dong S, Cui G (2021) Bioinspired antiaging binder additive addressing the challenge of chemical degradation of electrolyte at cathode/electrolyte interphase. J Am Chem Soc 143:18041
14. Yao Y, McDowell T, Ryu I, Wu H, Liu N, Hu L, Nix D, Cui Y (2011) Interconnected silicon hollow nanospheres for lithium-ion battery anodes with long cycle life. J Am Chem Soc 11:2949–2954
15. Buqa H, Holzapfel M, Krumeich F, Veit C, Novák P (2006) Study of styrene butadiene rubber and sodium methyl cellulose as binder for negative electrodes in lithium-ion batteries. J Power Sources 161:617–622
16. Chen Y, Zeng S, Qian J, Wang Y, Cao Y, Yang H, Ai X (2014) Li+ conductive polymer-embedded nano-Si particles as anode material for advanced Li-ion batteries. J Am Chem Soc 6:3508–3512
17. Markevich E, Salitra G, Aurbach D (2005) Influence of the PVDF binder on the stability of $LiCoO_2$ electrodes. Electrochem Commun 7:1298–1304
18. Yen J, Chang C, Lin Y, Shen S, Hong J (2013) Effects of styrene-butadiene rubber/carboxymethylcellulose (SBR/CMC) and polyvinylidene difluoride (PVDF) binders on low temperature lithium ion batteries. J Electrochem Soc 160:1811–1818
19. Liu Z, Dong T, Mu P, Zhang H, Liu W, Cui G (2022) Interfacial chemistry of vinylphenol-grafted PVDF binder ensuring compatible cathode interphase for lithium batteries. Chem Eng J 446:136798
20. Wei L, Chen C, Hou Z, Wei H (2016) Poly(acrylic acid sodium) grafted carboxymethyl cellulose as a high performance polymer binder for silicon anode in lithium ion batteries. Sci Rep 6:19583
21. Jeena M, Lee J, Kim S, Kim C, Kim J, Park S, Ryu J (2014) Multifunctional molecular design as an efficient polymeric binder for silicon anodes in lithium-ion batteries. J Am Chem Soc 6:18001–18007
22. Zhao H, Zhou X, Park S-J, Shi F, Fu Y, Ling M, Yuca N, Battaglia V, Liu G (2014) A polymerized vinylene carbonate anode binder enhances performance of lithium-ion batteries. J Power Sources 263:288–295
23. Grygiel K, Lee J, Sakaushi K, Antonietti M, Yuan J (2015) Thiazolium poly(ionic liquid)s: synthesis and application as binder for lithium-ion batteries. J Am Chem Soc 4:1312–1316
24. Tsao C, Hsu C, Kuo P (2016) Ionic conducting and surface active binder of poly(ethylene oxide)-block-poly(acrylonitrile) for high power lithium-ion battery. Electrochim Acta 196:41–47

25. Nguyen V, Kuss C (2020) Review—conducting polymer-based binders for lithium-ion batteries and beyond. J Electrochem Soc 167:065501
26. Zhu Y, Wang X, Hou Y, Gao X, Liu L, Wu Y, Shimizu M (2013) A new single-ion polymer electrolyte based on polyvinyl alcohol for lithium ion batteries. Electrochim Acta 87:113–118
27. Cao C, Li Y, Feng Y, Peng C, Li Z, Feng W (2019) A solid-state single-ion polymer electrolyte with ultrahigh ionic conductivity for dendrite-free lithium metal batteries. Energy Storage Materials 19:401–407
28. Zhang J, Wang S, Han D, Xiao M, Sun L, Meng Y (2020) Lithium (4-styrenesulfonyl) (trifluoromethanesulfonyl) imide based single-ion polymer electrolyte with superior battery performance. Energy Storage Mater 24:579–587
29. Dong T, Zhang H, Ma Y, Zhang J, Du X, Lu C, Shangguan X, Li J, Zhang M, Yang J, Zhou X, Cui G (2019) A well-designed water-soluble binder enlightening the 5 V-class $LiNi_{0.5}Mn_{1.5}O_4$ cathodes. Mater Chem A 7:24594–24601
30. Hergenrother P, Smith J (1994) Chemistry and properties of imide oligomers end-capped with phenylethynylphthalic anhydrides. Polymer 35:4857–4864
31. Ku J, Hwang S, Ham D, Song M, Shon J, Ji S, Choi J, Doo S (2015) Poly(isobutylene-*alt*-maleic anhydride) binders containing lithium for high-performance Li-ion batteries. J of Power Sources 287:36–42
32. Ryu S, Trapa P, Olugebefola S, Gonzalez-Leon J, Sadoway D, Mayes A (2005) Effect of counter ion placement on conductivity in single-ion conducting block copolymer electrolytes. J Electrochem Soc 152:A158–A163
33. Kwon N, Ryu S (2021) Synthesis and electrochemical properties of self-doped solid polymer electrolyte based on lithium 4-styrene sulfonate with BF_3-THF. Solid State Ionics 361:115563
34. Kelly J, Fafilek G, Besenhard O, Kronberger H, Nauer E (2005) Contaminant absorption and conductivity in polymer electrolyte membranes. J of Power Sources 145:249–252
35. Altava B, Compañ V, Andrio A, Castillo L, Mollá S, Burguete M, García-Verdugo E, Luis S (2015) Conductive films based on composite polymers containing ionic liquids absorbed on crosslinked polymeric ionic-like liquids (SILLPs). Polymer 72:69–81
36. Stoeva Z, Martin-Litas I, Staunton E, Andreev Y, Bruce P (2003) Ionic conductivity in the crystalline polymer electrolytes PEO_6:$LiXF_6$, X = P, As. Sb J Am Chem Soc 125:4619–4626
37. Zhou D, Shanmukaraj D, Tkacheva A, Armand M, Wang G (2019) Polymer electrolytes for lithium-based batteries: advances and prospects. Chem 5:2326–2352
38. He J, Wang J, Zhong H, Ding J, Zhang L (2015) Cyanoethylated carboxymethyl chitosan as water soluble binder with enhanced adhesion capability and electrochemical performances for $LiFePO_4$ cathode. Electrochim Acta 182:900–907
39. Hwang C, Cho Y, Kang N, Ko Y, Lee U, Ahn D, Kim J, Kim Y, Song H (2015) Selectively accelerated lithium ion transport to silicon anodes via an organogel binder. J of Power Sources 298:8–13
40. Nie M, Lucht B (2014) Role of lithium salt on solid electrolyte interface (SEI) formation and structure in lithium ion batteries. J Electrochem Soc 161:A1001–A1006
41. Wang A, Kadam S, Li H, Shi S, Qi Y (2018) Review on modeling of the anode solid electrolyte interphase (SEI) for lithium-ion batteries. Comput Mater 4:15
42. An S, Li J, Daniel C, Mohanty D, Nagpure S, Wood D III (2016) The state of understanding of the lithium-ion-battery graphite solid electrolyte interphase (SEI) and its relationship to formation cycling. Carbon 105:52–76
43. Pathan T, Rashid M, Walker M, Widanage W, Kendrick E (2019) Active formation of Li-ion batteries and its effect on cycle life. J Phys Energy 1:044003
44. An S, Li J, Du Z, Daniel C, Wood D III (2017) Fast formation cycling for lithium ion batteries. J of Power Sources 342:846–852